Journal of the Serbian Chemical Society
JSCS@tmf.bg.ac.rs • www.shd.org.rs/JSCS
J. Serb. Chem. Soc. *86* (11) 1053–1065 (2021)
JSCS–5482
Original scientific paper
Published 14 September 2021

The evaluation of chemoselectivity in multicomponent domino Knoevenagel/Diels–Alder reaction: A DFT study

MINA ATTARBASHI, NADER ZABARJAD SHIRAZ* and MARJANEH SAMADIZADEH

Department of Chemistry, Central Tehran Branch, Islamic Azad University, Tehran, Iran

(Received 29 January, revised 16 June, accepted 13 July 2021)

Abstract: Herein, the chemoselectivity of the multicomponent domino Knoevenagel/Diels–Alder reaction is investigated in terms of theoretical calculations. The structures of reagents, transition states, intermediates and products are optimized at the M062X/6-31+G(d,p) level of theory. The reaction mechanism involves processes of bond rotation, isomerization, asymmetric cycloaddition, acid–base and nucleophile–electrophile competitions, which are studied for the purpose of delivering a clear information of the mechanism in terms of chemoselectivity considerations. Accordingly, the chemoselectivity of the reaction is controlled by the releasing acetone during the decomposition of Meldrum acid in the presence of methanol and L-proline ($\Delta G^{\#}$ = 61.45 kcal** mol^{-1}). Comparing calculated results (gas and solvent phase) with the experimental ones showed that using these reagents are the kinetical favourite path for the chemoselective multicomponent cascade Knoevenagel/Diels–Alder reaction to produce the predominant product (>95 %). The results suggest that the creation of cis-spiro cyclohexanone is the predominant chemoselective product under kinetic control of the desired enone.

Keywords: theoretical study; cycloaddition; condensation reaction; cascade reaction.

INTRODUCTION

Due to the expedient access to complex polycyclic products in a single highly atom-economical step, multi-component coupling reactions (MCRS) mainly include simultaneous reactions of three or more reagents. MCRS make an easily achieved substituent diversity into the core structure by varying each component.[1,2]

The improvement of the reaction efficiency, the avoidance of toxic reagents, the reduction of waste, and the responsible use of our resources are critical con-

* Corresponding author. E-mail: zabarjad_sh@yahoo.com
https://doi.org/10.2298/JSC210119066A
** 1 kcal = 4184 J

cerns in modern synthetic organic chemistry.[3] Consisting of several bond-forming reactions, the domino or tandem reactions can solve many of these concerns. Domino reactions take place under the established common reaction conditions and are also involved with two or more bond-forming transformations.[4] Homo-domino reactions are classified as a combination of reactions involving the same mechanism, whereas heterodomino reactions are classified as a sequence of reactions with different mechanisms.[5]

As an ultimate goal in organic chemistry, the catalytic asymmetric assembly of simple and readily available precursor molecules, into stereochemically complex products, the name of domino reactions has become known.[6] Furthermore, the development of domino and other multicomponent reaction methodologies can provide a convenient admission to produce more complex compounds from simple starting materials.[2,7,8] The incorporation of a Diels–Alder reaction sequence is the fundamental key to many interesting variants of these reactions.[9–11]

Recently, organocatalysis has emerged as a promising synthetic tool for the constructing of C–C and C–N bonds in aldol,[12] Michael,[13] Mannich,[14] Diels––Alder[15] and other reactions[16] with very good chemoelectivity and stereoselectivity. In these recently described reactions, structurally simple and steady state of chiral organoamines enable iminium and enamine-based transformations with compounds containing carbonyl group. They could be used as catalysts in operationally simple and sometimes ecologically approachable experimental procedures.

Thus far, the extensive research have described the asymmetric assembly reactions involving aldol-aldol,[17–19] Michael-aldol,[20–22] Mannich-allylation,[23] Mannich-cyanation,[24,25] amination-aldol[26] and Knoevanagel–Michael[27] reactions. Recently, two motivating domino reactions were founded on Knoevenagel/Diels–Alder reaction sequences. The first was the direct organocatalytic asymmetric domino Knoevenagel/Diels–Alder reaction sequence, in order to accomplish the diastereo- and enantio-selective construction of highly substituted spiro [5.5]undecane-1,5,9-triones.[28] The second was the direct organocatalytic, hetero-domino, Knoevenagel/Diels–Alder/epimerization sequence with the intention to prepare symmetric prochiral and highly substituted spiro[cyclohexane--1,2′-indan]-1′,3′,4-triones in diastereospecific mode from the commercially existing 4-substituted 3-buten-2-ones, aldehydes and 1,3-indandione.[29]

In the synthesis of natural products and in materials chemistry, spirocyclic ketones are attractive intermediates[30,31] which are ideal starting materials for the synthesis of fenestranes, which could attend as uncommon designs for engineering of liquid crystal and chemistry science of dendrimers as well as for the building of the graphite cuttings in a saddle-like, 3D distorted core.[32,33] Additionally, the biphenyl moiety is an example of advantaged structure and this meets the priority of research in selecting biologically relevant chemical fragments, in

order to enhance the value of the resulting library as a source of bioactive compounds.[34]

The preliminary results (Scheme 1) indicated that the three-component reaction between benzylideneacetone **1**, aromatic aldehydes **2** and Meldrum acid **3** catalyzed by L-proline **4** resulted in some biologically active compounds of chiral spirocyclic ketone scaffolds **5** with excellent chemoselectivity (>95 %).[35]

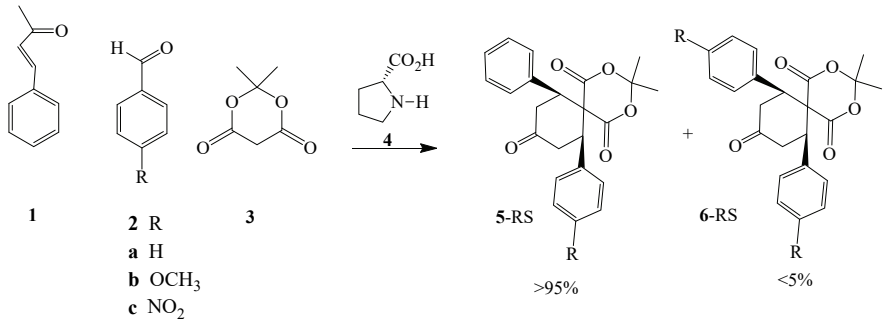

Scheme 1. Diastereoselective three-component reaction between benzylideneacetone **1**, aromatic aldehydes **2** and Meldrum acid **3** catalyzed by L-proline **4**.

The literature survey indicated that Knoevenagel/Diels–Alder has several distinct steps including Knoevenagel condensation and Diels–Alder cycloaddition, in which **5**-*RS* has been identified as a major product (Scheme S-1 in the Supplementary material to this paper). In the most reliable representation, Knoevenagel condensation occurs by reacting aldehyde **2** with Meldrum acid **3** in the presence of L-proline **4** as a catalyst to form alkylidene **8**. Simultaneously, diene **7** is formed through benzylideneacetone **1** and L-proline **4** condensation.[35]

Although there is much data about Knoevenagel condensation and Diels–Alder reaction individually, based on our survey of the literature, there are not sufficient theoretical studies concerning interpretation of chemoselectivity of Knoevenagel/Diels–Alder reaction. Recent increasing interest in domino Knoevenagel/Diels–Alder reaction, coupled with insufficient information concerning the clarification of the chemoselectivity of this reaction, was intended to study the chemoselectivity of domino Knoevenagel/Diels–Alder reaction. To extend the chemeoselectivity of Knoevenagel/Diels–Alder reaction, this research was initiated with the idea of selecting a suitable multi-component reaction that allows the efficient generation of structurally and stereochemically complex skeletons, bearing functionalities, which enable the attachment of the biasing elements. In the arena of multi-component reactions, we focused on the domino processes performance. We develop this theoretical study based on DFT calculations on how to interpret and predict the outcome of chemoselectivity, kinetic and

thermodynamic control of the Knoevenagel/Diels–Alder reaction in the presence of L-proline **4,** as a common chiral secondary amine catalyst.

THEORETICAL METHOD

Geometries of the structures were fully optimized with the internal 6-31+G(d,p) basis set, and DFT (M062X) method procedures implemented in Gamess software.[36] To choose the method and basis set, many factors need to be considered. Among several available methods/ /basis sets we use M06-2X/6-311+G(d,p) for following reasons. M06-2X/6-311+G(d,p) level of theory has been recommended for thermochemical data estimations including calculations that predict the ΔG values for the equilibria between enamines and ketones with the acceptable accuracy. The effect of solvent was studied by the polarizable continuum model (PCM) approaches and using M06-2X method with energy differences below 1 kcal mol^{-1}. Usually ordinary DFT methods (such as B3LYP) do not recognize the weak attraction between pairs of non-polar atoms and between pairs of molecules arising from the interaction of instantaneous multi-poles, but modern DFT methods, such as M06-2X are known to perform much better in the samw field.[37-40]

The frequency analysis were used in order to obtain the zero-point energies (ZPE), and confirmed the transition states with only one imaginary frequency and the reagents, intermediates, and products with zero imaginary frequency.[41] The starting materials and products were re-localized from the transition states by IRC calculations. Gibbs energy changes in a.u. (Hartree) were considered to compare relative stabilities (kcal mol^{-1}). The relative energy of transition states (**8**-TS, **7**-TS), intermediates (**8** and **7**) and products (**5** and **6**) were calculated by comparing their Gibbs energy change to the energy changes of relevant starting materials (Tables I–IV). The experimental findings showed that the reaction was facilitated by using methanol as a protic solvent. To survey the outcome of the reaction in a protic solvent, single--point calculations were accomplished at the same level of theory in PCM for methanol as a solvent. Gibbs energy changes in gas phase and solvent are presented in the Supplementary material file along with the Cartesian coordinates of optimized geometry of each structures.

RESULTS AND DISCUSSION

According to the experimental data, the domino Knoevenagel/Diels–Alder reaction progressed with an excellent chemoselectivity mode (>95 %) (Scheme 1).[35] To evaluate the results and the mechanism of the chemoselectivity, we reported the energy profile of this reaction by the quantum calculation on reagents, intermediates, transition states and all possible products involved in this reaction. Among various possibilities which are available for reagents (benzylideneacetone **1**, aldehyde **2**, Meldrum acid **3** and L-proline **4**) in order to to be in the reaction mixture, the reaction chooses the pathway that yields chemoselective Spirocyclic ketone **5**-*RS* in the presence of L-proline **4**. As shown in Scheme 1, the final product could have two isomers **5**-*RS* and **6**-*RS*. Although, *cis*-spiro-cyclohexanone **5**-*RS* was the main product of this reaction based on the experimental results. The chemoselectivity could happen through two possible steps.[35,42]

In this Diels–Alder reaction step *cis*-spiro **5**-*RS* and **6**-*RS* were produced through cyclization of diene **7** and dienophile **8**. Based on the obtained results, endo-Y orientation in **9**-*SR*-TS was a transition state, which passed through to

produce **9**-*RS*, and finally **5**-*RS* and/or **6**-*RS*. Based on the calculations, there were not considerable differences between $\Delta G^{\#}$ (kcal mol^{-1}) of these transition states that result in **6**-*RS* and **5**-*RS* as products (Table S-I, Supplemantary material).[42] Thus, according to the Diels–Alder reaction, both chemoselective products (**5** and **6**) were potentially capable to be produced in the reaction. Consequently, the Diels–Alder step could not control the observed experimental chemoselectivity of the reaction. In other word, it seems that this step may not be appropriate to explain the chemoselectivity of the reaction.

Knoevenagel condensation reaction step. In this reasonable step, diene **7** and dieneophile **8** were formed (Scheme S-1 in the Supplementary material). To study the chemoselectivity of the reaction, the ground states of reagents and components involved in the Knoevenagel step of domino Knoevenagel/Diels–Alder reaction were optimized at M062X/6-31+G(d,p) level of theory in gas, the Gibbs energy changes, and relative stabilities ($\Delta G^{\#}$) for components involved in the mechanism are summarized in Table I. The selected optimized geometries of the most stable structure of transition states were represented in Fig. S-1.

TABLE I. Energy of the relevant optimized transition states, intermediates, and dienophile **8** compared to Gibbs free energy of reagents in the gas phase for knoevenagel condensation

Formation of aldol **11**				Formation of dienophile **8**							
Addition step 4				E2 mechanism				E1 mechanism			
No.	ΔG / kcal mol^{-1}			No.	ΔG^4 / kcal mol^{-1}			No.	ΔG / kcal mol^{-1}		
R=	H	OCH_3	NO_2	R=	H	OCH_3	NO_2	R=	H	OCH_3	NO_2
10	0.00	0.00	0.00	**11**	3.37	6.74	-12.53	**11**	3.37	6.74	-12.53
3-TS	44.57	44.57	44.57	**12**-TS	62.22	59.76	57.39	**14**-TS1	56.05	44.43	60.00
3-enol	9.95	9.95	9.95	**13**-TS	56.44	67.27	53.94	**14**-Int	27.19	28.13	33.03
10-TS	46.82	49.18	38.29	**8**	0.76	17.79	26.41	**14**-TS2	79.76	75.77	77.16
11-Int	16.46	7.68	34.78					**8**	0.76	17.79	26.41
11-TS	29.64	17.21	68.30								
11	3.37	6.74	-12.53								

To prepare diene **7** and dienophile **8,** the reaction occured in several steps which are discussed in details.

1. Condensation of Meldrum acid **3** with aldehyde **2** to form dienophile **8**.
2. Degradation of dienophile **8** and releasing acetone **21** as a byproduct.
3. Aldol condensation of acetone **21** with aldehyde **2** to produce enone **29**.
4. Condensation of enone **29** with L-proline **4** to produce diene **7**.

*1. Condensation of Meldrum acid **3** with aldehyde **2** to form dienophile **8***

In this step, dienophile **8** was produced through the condensation reation between Meldrum acid **3** and aldehyde **2**. There was an alternative mechanism to explain this reaction in which Meldrum acid **3** was condensed with L-proline **4** to produce corresponding enamine in order to facilitate a condensation reaction to aldehyde **2**.[43] In this study the role of L-proline **4** role was ignored in the enol-

ization step in order to simplify the calculations, so the Scheme 2 was designed as Knoevenagel condensation reaction, in which Meldrum acid **3** enolized to **3**-enol ($\Delta G^{\#}$ = 9.95 kcal mol^{-1}) *via* **3**-TS ($\Delta G^{\#}$ = 44.57 kcal mol^{-1}). Intermediate **11** ($\Delta G^{\#}$ = 16.46 kcal mol^{-1}) was formed through **10**-TS ($\Delta G^{\#}$ = 46.82 kcal mol^{-1}) as a result of **3**-enol and aldehyde **2** addition reaction. The intermediate transferred an intermolecular proton (**11**-TS, $\Delta G^{\#}$ = 29.64 kcal mol^{-1}) to produce **11,** which was 3.37 kcal mol^{-1} more stable than the starting materials. In the next step, E1 or E2 mechanism was executed during the dehydration reaction to produce compound. E2 mechanism was performed by anti ($\Delta G^{\#}$ = 58.85 kcal mol^{-1}) or syn ($\Delta G^{\#}$ = 53.07 kcal mol^{-1}) mechanism. Comparison of the $\Delta G^{\#}$ of these reactions showed that the syn pathway had less activation energy compared to the anti-mechanism. The optimized structures of **12**-TS and **13**-TS demonstrated that the hydrogen bonding in **13**-TS could explain more stability of the transition state (Scheme S-2, Supplementary material, and Table I).

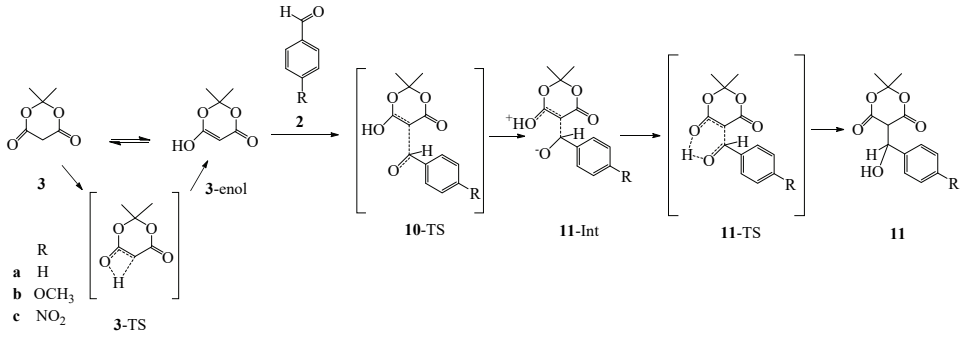

Scheme 2. Mechanism of Knoevenagel reaction to produce dienophile **8**.

Considering the E1 mechanism, **14-**Int carbocation ($\Delta G^{\#}$ = 27.19 kcal mol^{-1}) was formed through **14**-TS1 ($\Delta G^{\#}$ = 52.68 kcal mol^{-1}), and then it was converted to dienophile **8** by losing proton from **14**-TS2 ($\Delta G^{\#}$ = 52.57 kcal mol^{-1}). Consequently, E2 elimination with the syn orientation, passing through the least activation energy (53.07 kcal mol^{-1}), was preferred for the reaction. The electron withdrawing group (NO_2) stabilized aldol **11c**, while destabilized dienophile **8c** in comparison with corresponding starting materials.

*2. Degradation of dienophile **8** and releasing acetone **21** as a byproduct*

Enone **29**, which is considered as one of the compounds to produce isomer **6**, was formed during the condensation of acetone molecule **21** and aldehyde **2**. The required acetone could be released by a reaction between dienophile **8** and methanol (the solvent in the reaction). The released acetone was made by of methanol attacked to one of the carbonyl groups of compound **8** in order to produce intermediates **15** and **16** (Scheme 3), which were 54.23 and 46.63 kcal mol^{-1} less

stable than dienophile **8**, respectively. Hemi-orthoesters **17** and **18** were yielded through the proton transfer reaction of these intermediates (**15** and **16**). Next, the last intermediates were degraded in the presence of L-proline **4** through transition states **19** ($\Delta G^{\#}$ = 63.86 kcal mol^{-1}) and **20** ($\Delta G^{\#}$ = 61.45 kcal mol^{-1}) to produce acetone **21** and corresponding salt **22** (Table II, Fig. S-1).

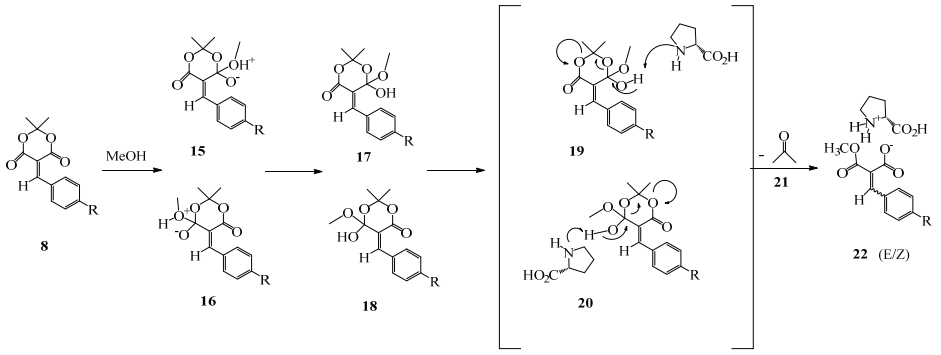

Scheme 3. Mechanism of acetone **21** production.

The comparison of relative energies showed that the departing of acetone **21** was the rate determining step of the degradation reaction (RDS, **20**, $\Delta G^{\#}$ = = 61.45 kcal mol^{-1}). The electron withdrawing NO_2 substituent increased $\Delta G^{\#}$ relatively (**19**c-TS and **20**c-TS) for about 8 kcal mol^{-1} when compared to the relevant substituted free derivatives (Table II).

TABLE II. $\Delta G^{\#}$ / kcal mol^{-1} of the relevant optimized transition states, intermediates and products compared to Gibbs energy changes of starting materials (**3**+**2**) in the gas phase for the formation of acetone

No.	R=			No.	R=		
	H	OCH_3	NO_2		H	OCH_3	NO_2
8	0.76	17.79	26.41	**8**	0.76	17.79	26.41
15	54.99	58.30	52.31	**16**	47.39	50.70	44.72
17	7.68	10.99	5.00	**18**	11.46	14.77	8.78
19-TS	71.54	74.09	79.27	**20**-TS	72.91	73.60	80.79
22-Z	–4.76	–1.45	–7.44	**22**-E	–9.09	–5.78	–11.77

*3. Aldol condensation of acetone **21** with aldehyde **2** to produce enone **29***

In this step, additional reaction of the produced acetone and aldehyde **2** conducted a reaction to form enone **29**. This reaction was similar to the knoevenagel condensation. The aldol condensation could be considered by the participating of L-proline **4** through enamine mechanism.[43] In this survey, an intermolecular enolization process was designed. According to our proposed mechanism, acetone **21** converted to **21**-enol ($\Delta G^{\#}$ = 12.05 kcal mol^{-1}) passing through **21**-TS

($\Delta G^{\#}$ = 56.11 kcal mol^{-1}, Scheme 4). **24**-Int ($\Delta G^{\#}$ = 19.67 kcal mol^{-1}) was formed through **23**-TS ($\Delta G^{\#}$ = 36.71 kcal mol^{-1}) by adding **21**-enol and aldehyde **2**, a proton transfer ($\Delta G^{\#}$ = 14.30 kcal mol^{-1}) of this zwitter-ion intermediate (**24**--TS) which led to *β*-hydroxy ketone **24** ($\Delta G^{\#}$ = 1.65 kcal mol^{-1}). In the final step, enon **29** was produced by a dehydration reaction, which could occurred by E2 and/or E1 mechanism (Scheme S-3, Supplementary material). Based on this assumption, there were four possible TS structures (**25**-TS, **26**-TS, **27**-TS and **28**--TS). For the E2 dehydration mechanism, it was necessary to consider the Pro-R and Pro-S hydrogens to perform either syn or anti-eliminations (Scheme 4, Table III). The lowest $\Delta G^{\#}$ of 48.98 kcal mol^{-1} belonged to **26**-TS in which Pro-S hydrogen was eliminated by the syn mechanism. Also, **26**-TS was in eclipsed conformation so that the aryl and the carbonyl groups were far from each other and hydrogen bonding in syn orientation provided a favoured TS for E2 elimination mechanism (Fig. S-1).

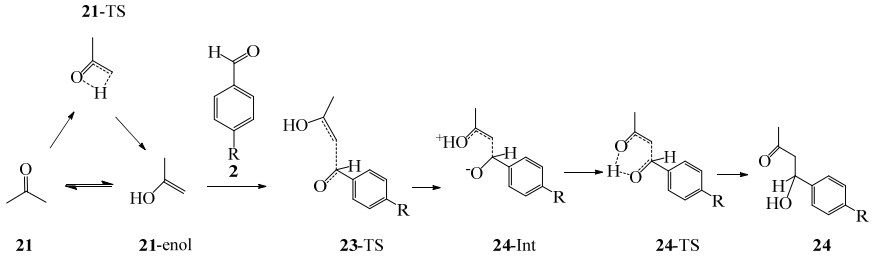

Scheme 4. Mechanism of aldol reaction to produce compound **22**.

TABLE III. $\Delta G^{\#}$ / kcal mol^{-1} of the relevant optimized transition states and product **29** compared to Gibbs energy changes of starting materials (**2**+**21**) in the gas phase for aldol condensation

Formation of aldol **24** Addition mechanism				Formation of enone **29**							
No.	R			No.	E2 Mechanism R			No.	E1 Mechanism R		
	H	OCH_3	NO_2		H	OCH_3	NO_2		H	OCH_3	NO_2
2+21	0	0	0	**24**	1.65	4.96	-1.18	**24**	1.65	4.96	-1.18
2+21-TS	56.11	56.11	56.11	**25**-TS	61.92	59.77	71.53	**30**-TS1	53.80	35.77	80.13
2+21-enol	12.05	12.05	12.05	**26**-TS	48.98	48.86	59.87	**31**-TS1	51.58	34.11	77.20
23-TS	48.76	55.23	29.16	**27**-TS	67.27	64.59	77.62	**32**-Int	19.67	8.54	22.69
24-Int	19.67	8.54	22.69	**28**-TS	64.96	64.23	76.14	**30**-TS2	57.33	45.74	27.03
24-TS	33.97	19.89	49.85	**29**-E	3.39	10.21	-11.38	**31**-TS2	54.67	44.32	22.95
24	1.65	4.96	-1.18	**29**-Z	16.37	15.15	-6.94	**29**-E	3.39	10.21	-11.38
								29-Z	16.37	15.15	-6.94

29-*E* was considered as a main product of this reaction, because it was 12.98 kcal mol^{-1} more stable than **29**-*Z* isomer. There were two possible transition state

structures (**30**-TS1, **31**-TS1), in E1 mechanism with $\Delta G^{\#}$ of 53.80 and 51.58 kcal mol^{-1}, respectively. So, the reaction chose the kinetically favourite pathway (**30**--TS1) to produce **32**-Int ($\Delta G^{\#}$ = 19.67 kcal mol^{-1}). In the next step, the proton could be removed by two transition states (**30**-TS2, $\Delta G^{\#}$ = 57.33 kcal mol^{-1}) and (**31**-TS2, $\Delta G^{\#}$ = 54.67 kcal mol^{-1}, Fig. S-1).

In this case, the reaction went through **30**-TS2 to produce enone **29**-*E*. By comparing $\Delta G^{\#}$ of the E1 and E2 mechanisms, the E2 mechanism *via* syn orientation ($\Delta G^{\#}$ = 48.98 kcal mol^{-1}) was accepted as the best pathway for dehydration reaction. The resulted enone **29**-*E* as the product of this step, proceeded a condensation reaction with L-proline **4** in the next step.

The results of calculations on the substituted reagents showed that $\Delta G^{\#}$ of **23**-TS was declined using an electron withdrawing group (NO_2) on aldehyde **2**. In the first step of the E1 mechanism, the electron releasing group (OCH_3) facilitated the OH^- departure and stabilized the cationic intermediate **32**-int, whereas the NO_2 group showed a contradictory effect on kinetic ($\Delta G^{\#}$) of this step. In the second step of the E1 mechanism the NO_2 group decreased $\Delta G^{\#}$ of deprotonation of transition states.

*4. Condensation of enone **29** with L-proline **4** to produce diene **7***

The intermediate **33** ($\Delta G^{\#}$ = 41.24 kcal mol^{-1}) was produced through the addition reaction between L-proline **4** and enone **1** and/or **29** (which was produced in previous step), this intermediate transferred a proton *via* **34**-TS ($\Delta G^{\#}$ = = 13.11 kcal mol^{-1}) to yield hemiaminal **35** ($\Delta G^{\#}$ = 37.79 kcal mol^{-1}) and was dehydrated by passing through an anti-oriented transition state **36**-TS ($\Delta G^{\#}$ = = 17.77 kcal mol^{-1}) to produce diene **7**. Among the different geometrical isomers and rotamers of **7**, the *trans*-s-*cis* **7** was the most stable isomer ($\Delta G^{\#}$ = 6.62 kcal mol^{-1}) and performed the Diels–Alder reaction with dienophile **8**. In terms of the effects of substitutes, the calculations demonstrated that all components bearing of NO_2 group, as an electron withdrawing group involved in this step, became more stable in comparison with the unsubstituted isomers (Scheme 5, Table IV).

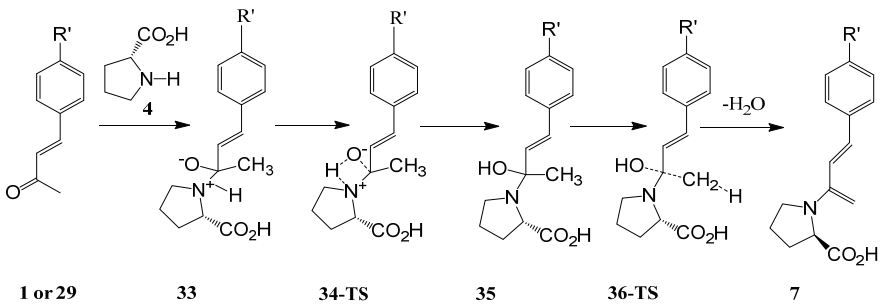

Scheme 5. Mechanism of producing diene **7**.

TABLE IV. $\Delta G^{\#}$ / kcal mol^{-1} of the relevant optimized transition states, intermediates and diene **7** compared to Gibbs energy changes of starting materials (**29**+**4**) in the gas phase

R	No.					
	29+**4**	**33**	**34**-TS	**35**	**36**-TS	**7**
H	0	41.24	54.35	37.79	55.56	6.62
OCH_3	0	43.81	58.54	41.65	59.99	1.75
NO_2	0	28.13	39.6	25.96	41.10	3.00

The optimized structure of **13**-TS showed that, leaving H^+ and OH^- groups were co-planar, and this dehydration step could be considered as a concerted reaction, but breaking of the C–H bond was more progressive (2.18 Å) than that of the C–O departing bond (1.65 Å). In **30**-TS2, the departing proton was located at 2.41 Å from the carbon atom and the conjugated system was almost planar, which made this transition state more stable. In **36**-TS, the C–H and C–O bonds were broken almost at the same extend, so the TS could be considered as a normal E2 transition state. On the other hand, of the formation of the O–H bond (2.32 Å) facilitated the dehydration of the molecule (Fig. S-1). Comparison of the calculations showed that the formation of product **6** required extra steps to complete the reaction. These steps, which led to diene **7,** included the acetone releasing step which could be considered as the rate determining step of the Knoevenagel reaction ($\Delta G^{\#}$ = 61.45 kcal mol^{-1}). In other words, this step caused a delay in the reaction to produce isomer **6**. To conclude, compound **5** as a chemoselective product was a product of the direct Diels–Alder reaction of ready to go available enone **1** with dienophile **8**.

Experimental findings showed that the reaction was promoted by the use of methanol as a protic solvent. Methanol as a protic solvent enhanced the reaction.[35] To survey the effect of protic solvent on kinetics of the reaction, the single-point calculations were conducted at the same level of theory in the polarizable continuum model (PCM) solvent utilizing methanol. The trend of the results in methanol was in agreement with the gas phase, all components involved in the mechanism were more stable in methanol in comparison to the gas phase. According to the calculations, Gibbs energies changes were decreased for 4–6 kcal mol^{-1} for the reagents and the products, 6–10 and 6–11 kcal mol^{-1} for the transition states and the intermediates, respectively, in the presence of methanol. Considering the polar solvent and polar character of transition states especially for the E1 mechanism, the product **8** proceeds *via* a polar transition state. The protic polar solvent (methanol) stabilized ionic intermediates **14**-Int and **32**-Int more than other reagents and transition states, and consequently declined the activation energy of the elimination step. As a consequence, activation energy of **14**-Int and **32**-Int have been decreased to 50.24 and 35.93 kcal mol^{-1}, respectively. The solvent effect is more considerable for reagents, transition states and

intermediates in Knoevenagel part of reaction, in comparison to Diels–Alder step for all substituents.

CONCLUSION

In summary, DFT calculations, especially in terms of chemoselectivity, provided a geometrical image of components involved in the Knoevanagel step in the multicomponent domino Knoevenagel/Diels–Alder reaction. The comparison of the calculated results with the experimental ones showed that using the active reagents has been kinetically the favourite pathway for the chemoselective multicomponent domino Knoevenagel/Diels–Alder reaction to produce **5**-RS as the predominant product (>95 %). Conversely, the reaction needed extra steps to produce the isomer **6**. These extra steps included the acetone releasing process, which was the rate determining step of the Knoevenagel reaction ($\Delta G^{\#}$ = 61.45 kcal mol^{-1}). Consequently, this difficult step caused a delay in the reaction to produce the product **6**. The solvent effect studies showed that methanol, as a polar protic solvent, declined the activation energy ($\Delta G^{\#}$), and promoted the reaction. In addition, the electron withdrawing group (NO_2) could accelerate the reaction to occur more convenient. It is worth noting that using the substituted enone **1** and adding acetone to the mixture of the reaction could affect the chemoselectivity of the reaction and still be a subject for future to research. This theoretical prediction may provide insights for researchers who are interested to design novel chemoselective products for the multicomponent domino Knoevenagel/Diels–Alder reactions considering desired substituents.

SUPPLEMENTARY MATERIAL

Additional data and information are available electronically at the pages of journal website: https://www.shd-pub.org.rs/index.php/JSCS/article/view/10333, or from the corresponding author on request.

ИЗВОД

ПРОЦЕНА ХЕМОСЕЛЕКТИВНОСТИ КОД МУЛТИКОМПОНЕТНЕ ДОМИНО KNOEVENAGEL/DIELS–ALDER РЕАКЦИЈЕ. DFT СТУДИЈА

MINA ATTARBASHI, NADER ZABARJAD SHIRAZ И MARJANEH SAMADIZADEH

Department of Chemistry, Central Tehran Branch, Islamic Azad University, Tehran, Iran

Овде је путем теоријских процена истраживана мултикомпонентна домино Knoevenagel/Diels–Alder реакција. Структуре реагенаса, прелазних стања и производа оптимизоване су на M062X/6-31+G(d,p) нивоу теорије. Механизам реакције укључује процесе ротације везе, изомерирацију, асиметричну циклоадицију, те киселинско–базна и нуклеофилно–електрофилна надметања, која су проучавана да би се добила јасна слика механизма у погледу разматрања хемоселективности. На основу тога, хемоселективност реакције је контролисана отпуштањем ацетона при разлагању Meldrum киселине у присуству метанола и l-пролина ($\Delta G^{\#}$ = 61,45 kcal/mol). Поређење израчунатих резултата са експерименталним показује да је коришћење ових реагенаса кинетички фаворизован пут за хемоселективну мултикомпонентну каскадну Knoevenagel/Diels–Alder реакцију

којом се добија главни производ (>95 %). Резултати показују да је *cis*-спиро-циклохексанона предоминантан хемоселективни производ под кинетичком контролом жељеног енона.

(Примљено 29. јануара, ревидирано 16. јуна, прихваћено 13. јула 2021)

REFERENCES

1. L. Reguera, D. G. Rivera, *Chem. Rev*. **119** (2019) 9836 (https://doi.org/10.1021/acs.chemrev.8b00744)
2. U. K. Sharma, P. Ranjan, E. V. Van der Eycken, S.-L. You, *Chem. Soc. Rev.* **49** (2020) 8721 (https://doi.org/10.1039/D0CS00128G)
3. R. C. Cioc, E. Ruijter, R. V. Orru, *Green Chem*. **16** (2014) 2958 (https://doi.org/10.1039/C4GC00013G)
4. H. Pellissier, *Adv. Synth. Catal.* **358** (2016) 2194 (https://doi.org/10.1002/adsc.201600462)
5. M. Ashe, *Master Thesis*, University of Southampton, Faculty of Natural and Environmental Sciences, Southampton, 2016 (http://eprints.soton.ac.uk/id/eprint/397980)
6. S. M. Xu, L. Wei, C. Shen, L. Xiao, H. Y. Tao, C. J. Wang, *Nat. Commun.* **10** (2019) 5553 (https://doi.org/10.1038/s41467-019-13529-z)
7. M. Wang, Z. Shi, *Chem. Rev.* **120** (2020) 7348 (https://doi.org/10.1021/acs.chemrev.9b00384)
8. H. A. Younus, M. Al. Rashida, A. Hameed, M. Uroos, U. Salar, S. Rana, K. M. Khan, *Expert Opin. Ther. Pat.* **31** (2021) 267 (https://doi.org/10.1080/13543776.2021.1858797)
9. X. Xiao, T. R. Hoye, *Nat. Chem.* **10** (2018) 838 (https://doi.org/10.1038/s41557-018-0075-y)
10. M. H. Cao, N. J. Green, S. Z. Xu, *Org. Biomol. Chem.* **15** (2017) 3105 (https://doi.org/10.1039/C6OB02761J)
11. X. Ji, C. Zhou, K. Ji, R. E. Aghoghovbia, Z. Pan, V. Chittavong, B. Ke, B. Wang, *Angew. Chem. Int. Ed.* **55** (2016) 15846 (https://doi.org/10.1002/anie.201608732)
12. Y. Yamashita, T. Yasukawa, W. J. Yoo, T. Kitanosono, S. Kobayashi, *Chem. Soc. Rev.* **47** (2018) 4388 (https://doi.org/10.1039/C7CS00824D)
13. J. Hu, M. Bian, H. Ding, *Tetrahedron Lett.* **57** (2016) 5519 (https://doi.org/10.1016/j.tetlet.2016.11.007)
14. J. F. Allochio Filho, B. C. Lemos, A. S. de Souza, S. Pinheiro, S. J. Greco, *Tetrahedron* **73** (2017) 6977 (https://doi.org/10.1016/j.tet.2017.10.063)
15. B. L. Oliveira, Z. Guo, G. J. L. Bernardes, *Chem. Soc. Rev.* **46** (2017) 4895 (https://doi.org/10.1039/C7CS00184C)
16. P. L. Wang, S. Y. Ding, Z. C. Zhang, Z. P. Wang, W. Wang, *J. Am. Chem. Soc.* **141** (2019) 18004 (https://doi.org/10.1021/jacs.9b10625)
17. W. Gati, H. Yamamoto, *Acc. Chem. Res.* **49** (2016) 1757 (https://doi.org/10.1021/acs.accounts.6b00243)
18. C. He, J. Hu, Y. Wu, H. Ding, *J. Am. Chem. Soc.* **139** (2017) 6098 (https://doi.org/10.1021/jacs.7b02746)
19. E. Sánchez-Larios, J. M. Holmes, C. L. Daschner, M. Gravel, *Org. Lett.* **12** (2010) 5772 (https://doi.org/10.1021/ol102685u)
20. J. Wang, H. Li, H. Xie, L. Zu, X. Shen, W. Wang, *Angew. Chem*. **119** (2007) 9208 (https://doi.org/10.1002/ange.200703163)
21. B. C. Hong, R. Y. Nimje, A. A. Sadani, J. H. Liao, *Org. Lett.* **10** (2008) 2345 (https://doi.org/10.1021/ol8005369)

22. W. Notz, F. Tanaka, C. F. Barbas, *Acc. Chem. Res.* **37** (2004) 580 (https://doi.org/10.1021/ar0300468)
23. A. Cordova, C. F. Barbas, *Tetrahedron Lett.* **44** (2003) 1923 (https://doi.org/10.1016/S0040-4039(03)00019-4)
24. F. Tanaka, C. F. Barbas III, *J. Syn. Org. Chem. Jpn.* **63** (2005) 709 (https://doi.org/10.5059/yukigoseikyokaishi.63.709)
25. S. Mukherjee, J. W. Yang, S. Hoffmann, B. List, *Chem. Rev.* **107** (2007) 5471 (https://doi.org/10.1021/cr0684016)
26. N. Campillo, J. A. Paez, P. Goya, *Helv. Chim. Acta* **86** (2003) 139 (https://doi.org/10.1002/hlca.200390003)
27. D. B. Ramachary, K. Anebouselvy, N. S. Chowdari, C. F. Barbas, *J. Org. Chem.* **69** (2004) 5838 (https://doi.org/10.1021/jo049581r)
28. R. Thayumanavan, B. Dhevalapally, K. Sakthivel, F. Tanaka, C. F. Barbas III, *Tetrahedron Lett.* **43** (2002) 3817 (https://doi.org/10.1016/S0040-4039(02)00686-X)
29. N. S. Chowdari, C. F. Barbas, *Org. Lett.* **7** (2005) 867 (https://doi.org/10.1021/ol047368b)
30. E. M. Carreira, T. C. Fessard, *Chem. Rev.* **114** (2014) 8257 (https://doi.org/10.1021/cr500127b)
31. L. Hong, R. Wang, *Adv. Synth. Catal*. **355** (2013) 1023 (https://doi.org/10.1002/adsc.201200808)
32. J. Tellenbröker, D. Kuck, *Eur. J. Org. Chem.* **2001** (2001) 1483 (https://doi.org/10.1002/1099-0690(200104)2001:8<1483::AID-EJOC1483>3.0.CO;2-U)
33. A. Boudhar, M. Charpenay, G. Blond, J. Suffert, *Angew. Chem. Int. Ed.* **52** (2013) 12786 (https://doi.org/10.1002/anie.201304555)
34. L. Porcelli, D. Stolfa, A. Stefanachi, R. Di Fonte, M. Garofoli, R. Iacobazzi, N. Silvestris, A. Guarini, S. Cellamare, A. Azzariti, *Cancer Lett.* **445** (2019) 1 (https://doi.org/10.1016/j.canlet.2018.12.013)
35. D. B. Ramachary, C. F. Barbas III, *Chem. Eur. J.* **10** (2004) 5323 (https://doi.org/10.1002/chem.200400597)
36. M. W. Schmidt, K. Baldridge, J. A. Boatz, S. T. Elbert, M. S. Gordon, J. H. Jensen, S. Koseki, N. Matsunaga, K. A. Nguyen, S. Su, T. L. Windus, M. Dupuis, J. A. Montomery, *J. Comput. Chem*. **14** (1993) 1347 (https://doi.org/10.1002/jcc.540141112)
37. Y. Zhao, D. G. Truhlar, *Theor. Chem. Acc*. **120** (2008) 215 (https://doi.org/10.1007/s00214-007-0310-x)
38. A. Castro-Alvarez, H. Carneros, D. Sanchez, J. Vilarrasa, *J. Org. Chem*. **80** (2015) 11977 (https://doi.org/10.1021/acs.joc.5b01814)
39. M. Head-Gordon, J. A. Pople, M. J. Frisch, *J. Chem. Phys. Lett*. **153** (1988) 503 (https://doi.org/10.1016/0009-2614(88)85250-3)
40. Y. Zhao, N. E. Schultz, D. G. Truhlar, *J. Chem. Phys*. **123** (2005) 161103 (https://doi.org/10.1063/1.2126975)
41. S. B. Trickey, *Int. J. Quantum Chem*. **59** (1996) 259 (https://doi.org/10.1002/qua.560590302)
42. M. Attarbashi, N. Zabarjad Shiraz, M. Samadizadeh, *J. Theor. Comput. Chem.* **19** (2020) 2050005 (https://doi.org/10.1142/S0219633620500054)
43. M. Girod, B. Grammaticos, *Nucl. Phys., A* **330** (1979) 40 (https://doi.org/10.1016/0375-9474(79)90535-9).